30th International Conference
ENGINEERING MECHANICS 2024
Milovy, Czech Republic, May 14 – 16, 2024

MODELLING OF LEADING EDGE MORPHING BY USING GEOMETRICALLY EXACT BEAM THEORY

Hrstka M.[*], **Bajer J.**[**], **Hadaš Z.**[***], **Sharif Khodaei Z.**[†], **Aliabadi F.**[††], **Kotoul M.**[†††]

Abstract: *The goal of the presented work is to demonstrate a capability of a non-linear computational model for a leading edge morphing based on the geometrically exact Timoshenko beam theory implemented in the finite element method. The leading edge topology is divided into outer surface with various bending and tension response along the element centre line and kinematic mechanism. Their interconnection is realized by joints, in the computational model realized by the Lagrange multiplier technique. Loading is realized by prescribed moment in one mounting node which represents an electric servomotor. In the results section, beam resultants dependent on the various initial configuration of the kinematic mechanism are analysed.*

Keywords: Morphing wing, geometrically exact beam, finite element method, non-linear analysis, Lagrange multiplier method, meta-materials.

1. Introduction

Wing morphing has been used in aeronautical engineering since the Wright brothers controlled the course of their Flyer by manually manipulating wing surfaces. Generally, wing morphing is a concept of the airfoil shape modification in order to improve aerodynamic properties and system performance over the aircraft's nominal flight envelope. There are various morphing concepts, such as camber or wingspan modifications, active twist or sweep changes. The presented study is focused on the leading edge morphing of one wing segment, where the construction on the airfoil includes three main parts – a central box, a leading edge and a trailing edge (see Fig. 1a). There are numerous approaches dealing with wing morphing, e.g. topological optimization Gu et al. (2021); Achleitner et al. (2019); Dexl et al. (2020) or design of a kinematic mechanism with non-zero degrees of freedom Li et al. (2022); Sun et al. (2022). The usage of classical materials in aeronautical engineering as aluminium alloys or Duralumin are limited by bending deflection which relies on the yield strength and the cross section thickness. This is sometimes in contrast with other requirements, e.g. with ability to withstand aero-static and aerodynamic loads and with bending rigidity or buckling. This contradictory requirements can be treated by using meta-material structures with mechanical properties that can be tailored according to the operational conditions, Olympio and Gandhi (2010a,b). This work focuses on the design of the kinematic mechanism (the topology and functional principle is depicted in Fig. 1c) by using simplified geometrically exact beam model where the non-linear problem is solved by the finite element method, based on the studies of Reissner (1972); Simo (1985); Wood and Zienkiewicz (1977).

[*] Ing. Miroslav Hrstka, PhD.: Institute of Solid Mechanics, Mechatronic and Biomechanics, Brno University of Technology, Technická 2896/2; 616 69, Brno; CZ, miroslav.hrstka1@vutbr.cz

[**] Ing. Jan Bajer: NCC MESTEC - Cybernetics and Robotics Division, Brno University of Technology, Technická 2896/2; 616 69, Brno; CZ, Jan.Bajer@vutbr.cz

[***] Assoc. Prof. Zdeněk Hadaš, PhD.: Institute of Automation and Computer Science, Brno University of Technology, Technická 2896/2; 616 69, Brno; CZ, hadas@fme.vutbr.cz

[†] Prof. Zahra Sharif Khodaei, PhD.: Department of Aeronautics, Imperial College London, Exhibition Rd, SW7 2AZ South Kensington, London, UK, z.sharif-khodaei@imperial.ac.uk

[††] Prof. M H Ferri Aliabadi, FRAeS, FIMA, CEng, CMaths: Department of Aeronautics, Imperial College London, Exhibition Rd, SW7 2AZ South Kensington, London, UK, m.h.aliabadi@imperial.ac.uk

[†††] Prof. RNDr. Michal Kotoul, DSc.: Institute of Solid Mechanics, Mechatronic and Biomechanics, Brno University of Technology, Technická 2896/2; 616 69, Brno; CZ, kotoul@fme.vutbr.cz

doi: 10.21495/em2024-134

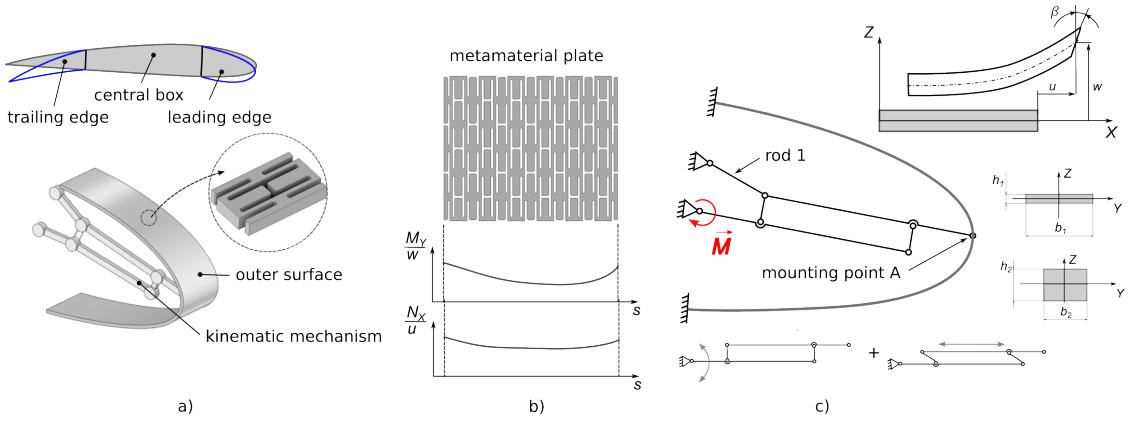

Fig. 1: a) NACA 2412 airfoil and leading edge geometry and mechanism illustration, b) meta-material plate with varying cell bending response, c) wire model of the morphing wing assembly.

2. Methods

Implementing meta-materials in the morphing wing design requires multi-disciplinary modelling approach due to the generally anisotropic and heterogeneous behaviour of these structures. They are valuable for their large bending flexibility. An example of such meta-material in shown in Fig. 1b. The graphs below show dependence of the bending and tensional stiffness along the meta-material plate. Thus, when a optimization is used to find an optimal material properties of the outer surface and topology of the kinematic mechanism dependent on the prescribed external loading, it is convenient to find a suitable simplification of the computational model to speed-up the process and suppress the model quantities that can be designed afterwards.

The presented computational model deals with morphing of the the leading edge. The wing segment geometry is depicted in Fig. 1c. The leading edge is simplified into two regions - the outer surface and the kinematic mechanism, mounted at the central box.

The solution process of the design loop within the BAANG project and resides in determination of the optimal material properties, i.e. a bending and axial stiffness of the outer surface and topology of the kinematic mechanism and its mounting points position according to the desired morphed airfoil shape resulting from the aero-elastic optimization. The presented study represent the initial part, i.e. determination of the mechanical response.

The mechanical behaviour of both outer surface and kinematic mechanism are simulated with the finite element method (FEM) by using geometrically exact Timoshenko beam and finite strain theory, as the nominal deflections are significant. Let us consider a leading edge geometry in the X-Z plane represented by beams with material parameters and geometry of the cross section (see Fig. 1c). No out-plane loading is considered. The geometry is meshed with the prescribed element length. Every element is then represented by a straight beam spatially oriented in the reference coordinate system X-Z. Motion of the beam to the deformed coordinate system (denoted by x-z) is described in Simo (1985); Reissner (1972)

$$x = X + u(X) + Z\sin\beta(X), \quad y = Y, \quad z = w(X) + Z\cos\beta(X), \tag{1}$$

where $u(X)$, $w(X)$ are axial deformation and deflection in the reference coordinate system and $\beta(X)$ is the cross section rotation. The deformation gradient, the Green-Lagrange strain tensor and the second Piola-Kirchhoff stresses are computed as

$$F_{iI} = \begin{bmatrix} [1 + u_{,X} + Z\beta_{,X}\cos\beta] & 0 & \sin\beta \\ 0 & 1 & 0 \\ [w_{,X} - Z\beta_{,X}\sin\beta] & 0 & \cos\beta \end{bmatrix}, \quad \mathbf{E} = \frac{1}{2}(\mathbf{F}^T\mathbf{F} - \mathbf{I}), \quad \mathbf{S} = \frac{1}{\det(\mathbf{F})}\mathbf{F}^{-1}\sigma\mathbf{F}^{-T}. \tag{2}$$

Where $(,X)$ is the derivative with respect to the coordinate X and σ is the Cauchy stress. There are only two non-zero components of (2c), i.e.

$$\begin{aligned} E_{XX} &= u_{,X} + \frac{1}{2}(u_{,X}^2 + w_{,X}^2) + Z\Lambda\beta_{,X} = E_0 + ZK^{\mathrm{b}}, \\ 2E_{XZ} &= (1 + u_{,X})\sin\beta + w_{,X}\cos\beta = \Gamma, \quad \Lambda = (1 + u_{,X})\cos\beta - w_{,X}\sin\beta. \end{aligned} \tag{3}$$

The variational form for the beam can be written as

$$\delta\Pi = \int_\Omega (\delta E_{XX} S_{XX} + 2\delta E_{XZ} S_{XZ}) \mathrm{d}V - \delta\Pi_{\mathrm{ext}}, \tag{4}$$

where $\delta\Pi_{\mathrm{ext}}$ is the variation of external forces. By considering a quadratic three-node element, the finite element approximation for the displacements and their shape functions for nodes $a = 1, 2, 3$ are

$$\begin{Bmatrix} u \\ w \\ \beta \end{Bmatrix} = N_a(X) \begin{Bmatrix} \hat{u}_a \\ \hat{w}_a \\ \hat{\beta}_a \end{Bmatrix}, \quad N_1 = \frac{1}{2}\xi(1-\xi),\ N_2 = 1-\xi^2,\ N_3 = \frac{1}{2}\xi(1+\xi),\ \xi \in < -1, 1 > . \tag{5}$$

Performing the standard linearization of the non-linear weak form, the problem can be written in the incremental form as

$$\mathbf{K}_{\mathrm{T}} \mathrm{d}\mathbf{u} = \Psi(\mathbf{u}) = -(\mathbf{f}_{\mathrm{int}} - \mathbf{f}_{\mathrm{ext}}), \tag{6}$$

where $\mathbf{f}_{\mathrm{int}}$, $\mathbf{f}_{\mathrm{ext}}$ are internal and external forces, respectively. The tangent stiffness matrix is defines as

$$(\mathbf{K}_{\mathrm{T}})_{ab} = \int_L \mathbf{B}_a^T \mathbf{D}_T \mathbf{B}_b \, \mathrm{d}X + (\mathbf{K}_{\mathrm{G}})_{ab}, \quad (\mathbf{K}_{\mathrm{G}})_{ab} = \int_\Omega \frac{\partial \mathbf{B}_a}{\partial \mathbf{u}} \sigma_b \, \mathrm{d}V, \quad \mathbf{u} = \begin{Bmatrix} u \\ w \\ \beta \end{Bmatrix}, \tag{7}$$

where

$$\mathbf{D}_{\mathrm{T}} = \begin{bmatrix} EA & 0 & 0 \\ 0 & \kappa GA & 0 \\ 0 & 0 & EI \end{bmatrix}, \quad \mathbf{B}_a = \begin{bmatrix} (1+u_{,X})N_{a,X} & w_{,X}N_{a,X} & 0 \\ \sin\beta N_{a,X} & \cos\beta N_{a,X} & \Lambda N_a \\ \beta_{,X}\cos\beta N_{a,X} & -\beta_{,X}\sin\beta N_{a,X} & (\Lambda N_{a,X} - \Gamma\beta_{,X} N_a) \end{bmatrix}, \tag{8}$$

where the Saint-Venant material type is considered and E is the Young modulus, G is the shear modulus, I is the second moment of inertia of the cross section and A is the cross section area. The expression of the geometric stiffness matrix $\mathbf{K}_{\mathrm{G}}$ can be found in Zienkiewicz and Taylor (2005), Chapter 17.

The non-linear equation (6) was solved by the Newton-Raphson method and accelerated by the line-search technique, where the i-th iteration factor η_i in $\mathbf{u}_{i+1} = \mathbf{u}_i + \eta_i \mathrm{d}\mathbf{u}_i$ is determined in order to minimize the projection

$$G_i \equiv (\mathrm{d}\mathbf{u}_i)^T \mathbf{\Psi}(\mathbf{u}_i + \eta_i \mathrm{d}\mathbf{u}_i) = 0. \tag{9}$$

Since the geometry is generally spatially oriented, the element quantities have to be transformed to the global coordinate system by standard transformation relations (see Zienkiewicz and Taylor (2005). Governing matrices of the system are then assembled by using

$$\mathbf{K}_T^s = \sum_{\mathrm{elements}} \mathbf{K}_T^g, \quad \mathbf{f}_{\mathrm{int}}^s = \sum_{\mathrm{elements}} \mathbf{f}_{\mathrm{int}}^g. \tag{10}$$

Both outer surface and kinematic mechanism are represented by beam elements with defined parameters. Their interconnection is modelled by the Lagrange multiplier technique. In the connection nodes, the degrees of freedom u and w are coupled, by which a revolute kinematic pair is simulated. Equation (6) is expanded to the form of

$$\begin{bmatrix} \mathbf{K}_T + \lambda_a \mathbf{H}_a & \mathbf{G}^T \\ \mathbf{G} & \mathbf{0} \end{bmatrix} \begin{Bmatrix} \mathrm{d}u \\ \mathrm{d}\lambda \end{Bmatrix} = \begin{Bmatrix} -(\mathbf{f}_{\mathrm{int}} - \mathbf{f}_{\mathrm{ext}}) - \lambda^T \mathbf{G} \\ -\mathbf{g} \end{Bmatrix}, \quad \mathbf{f}_{\mathrm{int}} = \int_L \mathbf{B}_a^T \mathbf{S} \, \mathrm{d}X, \quad a = 1, 2, 3$$
$$g_X = u_a - u_b, \quad g_Z = w_a - w_b, \quad G_I = \frac{\partial g_I}{\partial u_a}, \quad H_I = \frac{\partial^2 g_I}{\partial u_a \partial u_b}, \quad I = 1, 2, ..., n_c, \quad n_c \text{ is the node count.} \tag{11}$$

3. Results

The capabilities of the presented model were tested on three cases of the rod 1 mounting position (see Fig. 1c). Initial geometry and deformation of the case 1, case 2 and case 3 are depicted in Fig. 2a. Input parameters were $E = 200$ GPa, $\mu = 0.3$, $G = E/(2(1+\mu))$, $b_1 = 20$ mm, $h_1 = 1$ mm, $b_2 = 5$ mm, $h_2 = 5$ mm, $\kappa = 5/6$, $I = bh^3/12$. The kinematic mechanism is loaded by the moment $M = 2$ Nm. The FEM model has 70 quadratic elements and 147 nodes. The beam resultants are depicted in Fig. 2. The axial force N_x, shear force T_z and bending moment M_o are computed from the integral (11) and are mapped to the deformed geometry. It can be seen that the character of the beam resultants can be governed by changing the position the rod 1, setting the relative motion of the mounting point A to positive or negative (causing compression or tension in the beam).

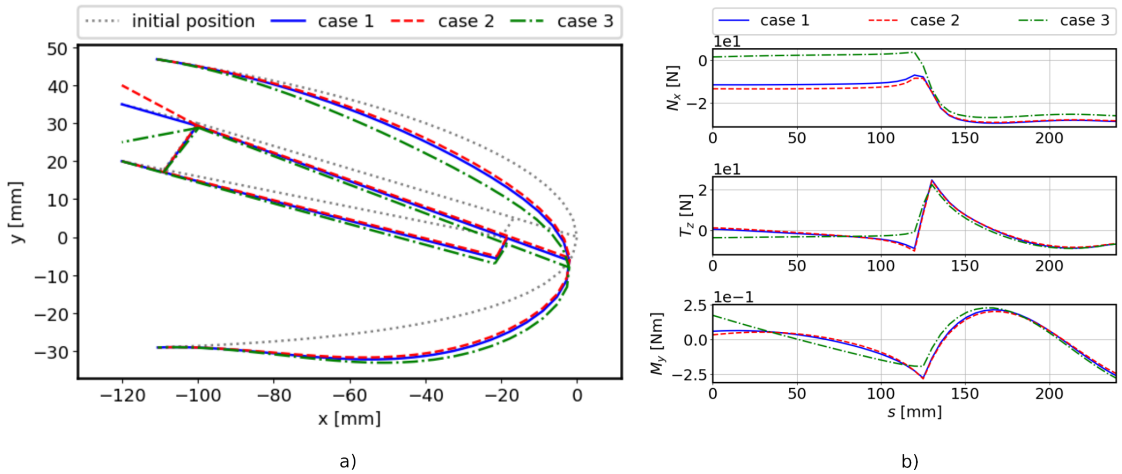

Fig. 2: a) The initial geometry and deformations of three rod 1 mounting positions, b) beam resultants: axial force N_x, shear force T_z, bending moment M_y mapped on the deformed geometry.

4. Conclusions

The geometrically exact beam theory applied to the problem on the leading edge morphing has been investigated. The main goal of the paper was to prove the capability and parametrization of the computational algorithm for future optimization of the material parameters and desired morphed outer surface position as a output from aero-elastic analysis. Also solving methods of the non-linear finite element method were implemented, as line-search technique for the Newton-Raphson method. Nevertheless, the parameters in the material matrix (8) are to be modified in the subsequent work according to he meta-material response, as is depicted in Fig. 1b.

Acknowledgment

Computational resources were provided by the e-INFRA CZ project (ID:90254), supported by the Ministry of Education, Youth and Sports of the Czech Republic. The authors acknowledge the supports by Horizon Europe via the project HORIZON-WIDERA-2021-ACCESS-03, SEP-210806308.

References

Achleitner, J., Rohde-Brandenburger, K., von Bieberstein, P. R., Sturm, F., and Hornung, M. (2019) Aerodynamic design of a morphing wing sailplane. *AIAA Aviation 2019 Forum*.

Dexl, F., Hauffe, A., and Wolf, K. (2020) Multidisciplinary multi-objective design optimization of an active morphing wing section. *Structural and Multidisciplinary Optimization*, 62, 5, pp. 2423–2440.

Gu, X., Yang, K., Wu, M., Zhang, Y., Zhu, J., and Zhang, W. (2021) Integrated optimization design of smart morphing wing for accurate shape control. *Chinese Journal of Aeronautics*, 34, 1, pp. 135–147.

Li, Y., Ge, W., Zhou, J., Zhang, Y., Zhao, D., Wang, Z., and Dong, D. (2022) Design and experiment of concentrated flexibility-based variable camber morphing wing. *Chinese Journal of Aeronautics*, 35, 5, pp. 455–469.

Olympio, K. R. and Gandhi, F. (2010a) Flexible skins for morphing aircraft using cellular honeycomb cores. *Journal of Intelligent Material Systems and Structures*, 21, 17, pp. 1719–1735.

Olympio, K. R. and Gandhi, F. (2010b) Zero poisson's ratio cellular honeycombs for flex skins undergoing one-dimensional morphing. *Journal of Intelligent Material Systems and Structures*, 21, 17, pp. 1737–1753.

Reissner, E. (1972) On one-dimensional finite-strain beam theory: The plane problem. *Zeitschrift für angewandte Mathematik und Physik ZAMP*, 23, 5, pp. 795–804.

Simo, J. C. (1985) A finite strain beam formulation. The three-dimensional dynamic problem. Part I. *Computer Methods in Applied Mechanics and Engineering*, 49, 1, pp. 55–70.

Sun, J., Li, X., Xu, Y., Pu, T., Yao, J., and Zhao, Y. (2022) Morphing Wing Based on Trigonal Bipyramidal Tensegrity Structure and Parallel Mechanism. *Machines*, vol. 10.

Wood, R. D. and Zienkiewicz, O. C. (1977) Geometrically nonlinear finite element analysis of beams, frames, arches and axisymmetric shells. *Computers & Structures*, 7, 6, pp. 725–735.

Zienkiewicz, O. C. and Taylor, R. (2005) *Finite Element Method for Solids and Structural Mechanics*. Elsevier B. H., Burlington, 6th edition.